Ross Sea NBP VM-ADCP Analyses (L. Padman, ESR)

Principal tasks (approximate ESR %effort in brackets)

(40%) Tidal inverse modeling: Tides are the dominant signal in upper-ocean currents in Ross Sea models and measurements. Therefore, our first task is to evaluate tides. We do this by assimilation of all NBP VM-ADCP data.

(20%) Compare detided VM-ADCP with modeled subtidal currents; NW Ross Sea, McMurdo Sound, Ross Ice Shelf front.

(25%) Use of VM-ADCP for studies of Antarctic Slope Front (ASF): relationship to topography, and cross-slope scales.

(10%) Assist Stanford University senior Isabella Arzeno with her undergraduate thesis research on Ross Ice Shelf near-front tidal currents. Isabella began this project as a summer REU intern with Bob Beardsley (WHOI), working on ANDRILL 2010 oceanographic mooring data from the RIS front.

(5%) Miscellaneous explorations, e.g.: space scales of fronts in the Pacific sector of the Southern Ocean, baroclinicity.

Principal Conclusions

1. The distribution of upper-ocean current speed measured by VM-ADCP speed is highly heterogeneous. Large values are found along the shelf break, particularly in the NW corner near the northern end of Drygalski Trough and Cape Adare, where <u>mean</u> speeds exceed 0.4 m s^{-1}. Large values are also found along the Pennell and Iselin banks, over the northern end of Ross Bank, and intermittently along the Ross Ice Shelf front. Except for the last region, strong currents in the upper-ocean VM-ADCP record correspond to regions of significant tidal currents.

2. The large Ross Sea data set from the vessel-mounted ADCP (VM-ADCP) on *Nathaniel B. Palmer* (NBP) provides significant improvements in current velocity predictions from assimilative tide models. These models are now routinely used to detide VM-ADCP and lowered ADCP (LADCP) records, and to evaluate tidal impacts on other processes including sea ice formation, ice-shelf basal melt, and Antarctic Bottom Water (AABW) production.

3. The ability to accurately detide NBP VM-ADCP records allows us to identify topographically constrained flows over the Ross Sea continental shelf. These flows are predicted in 3-D ocean models, and are critical to the provision of ocean heat to the Ross Ice Shelf, and export of dense shelf water to the shelf break.

4. VM-ADCP records allow us to identify preferred forcing sets for numerical models of Ross Sea oceanography and sea ice (and sub-ice-shelf basal melting). In general, we conclude that the medium-resolution regional Antarctic Mesoscale Prediction System (AMPS) is better than the global coarse-grid reanalysis model ERA-Interim, and that adding tides makes a significant difference to time-averaged (seasonal presented here) upper-ocean velocities, presumably through changes in mixing rates on the continental shelf.

5. Currents are remarkably barotropic. In a survey of the entire data set, very few observations showed significant shear. This is in contrast to some records from the

Bellingshausen Sea [*Howard et al*., 2004], which showed dramatic near-inertial shear across the pycnocline. The barotropic nature of Ross Sea currents may reflect the weaker stratification there, or that the surface mixed layer is too thin in summer (the time of most NBP cruises) to be resolved by the NBP 150 kHz VM-ADCP.

Distribution of currents

Figure 1 shows the distribution of mean upper-ocean (50-350 m) ADCP speed $|\mathbf{u}|_{VM}$ from all NBP VM-ADCP data. $|\mathbf{u}|_{VM}$ is calculated as the mean of sqrt(u^2+v^2), where u and v are east and north velocity components. Values >0.5 m s^{-1} are found along the NW Ross Sea shelf break, and other regions of large $|\mathbf{u}|_{VM}$ occur over the banks of the central Ross Sea and Iselin Bank, which extends north of the main trend of the shelf break. Intermittent, moderate values are also found close to the Ross Ice Shelf front. A comparison with **Figure 2** (a map of modeled barotropic tidal currents) shows that these region of large $|\mathbf{u}|_{VM}$ are strongly correlated with tidal currents. We assume that most cruises are randomly sampling tidal currents; while areas of sparse data coverage may be biased by tidal state at the time of each cruise, overall the map indicates reasonable sampling of tides.

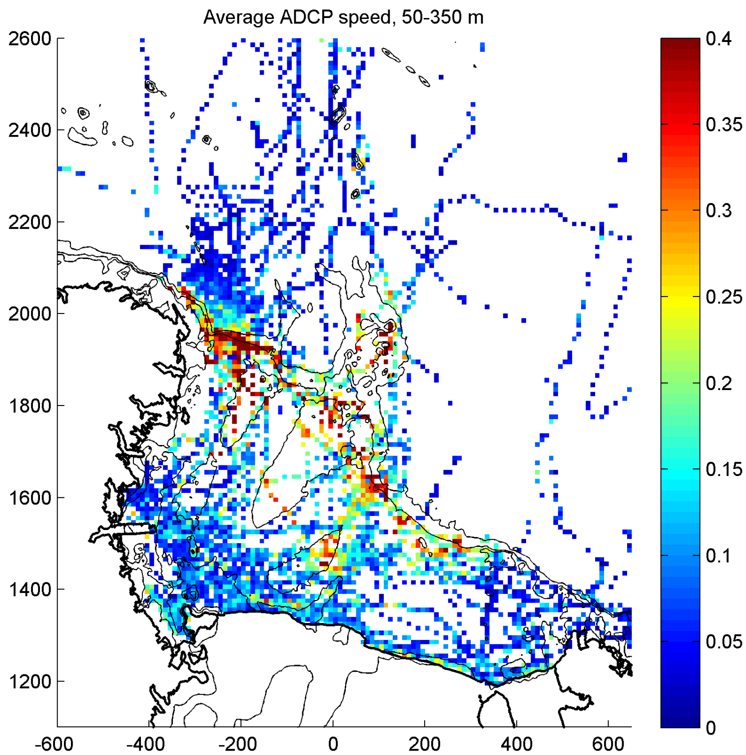

Figure 1: *Map of average speed measured by the NBP VM-ADCP ($|\mathbf{u}|_{VM}$: m s^{-1}) evaluated for the depth range 50-350 m and in 10x10 km bins.*

Tide modeling

We have been upgrading tide models for Antarctica, and some regional solutions for the Ross Sea, for many years [*Padman et al*., 2002, 2003, 2008; *Padman and Fricker*, 2005]. These models have included dynamics-based (forced at boundaries and through the astronomical potentials) models, as well as inverse models primarily with assimilation of surface (ocean and ice shelf) elevation data. The maximum modeled tidal current speeds (**Fig. 2**) are in the NW Ross Sea, with values occasionally exceeding 1 m s^{-1}. These currents have profound implications for export of dense shelf water and associated production of Antarctic Bottom Water (AABW) [*Padman et al*., 2009; *Budillon et al*. (incl. Padman), 2011].

These tidal currents are large compared with mean flows (with the exception of benthic outflows of dense shelf water that are not sampled by VM-ADCP). Thus, developing the accuracy of models of tidal currents is an essential step towards measuring mean flows and validating models such as those by *Dinniman et al.* [2007, 2010].

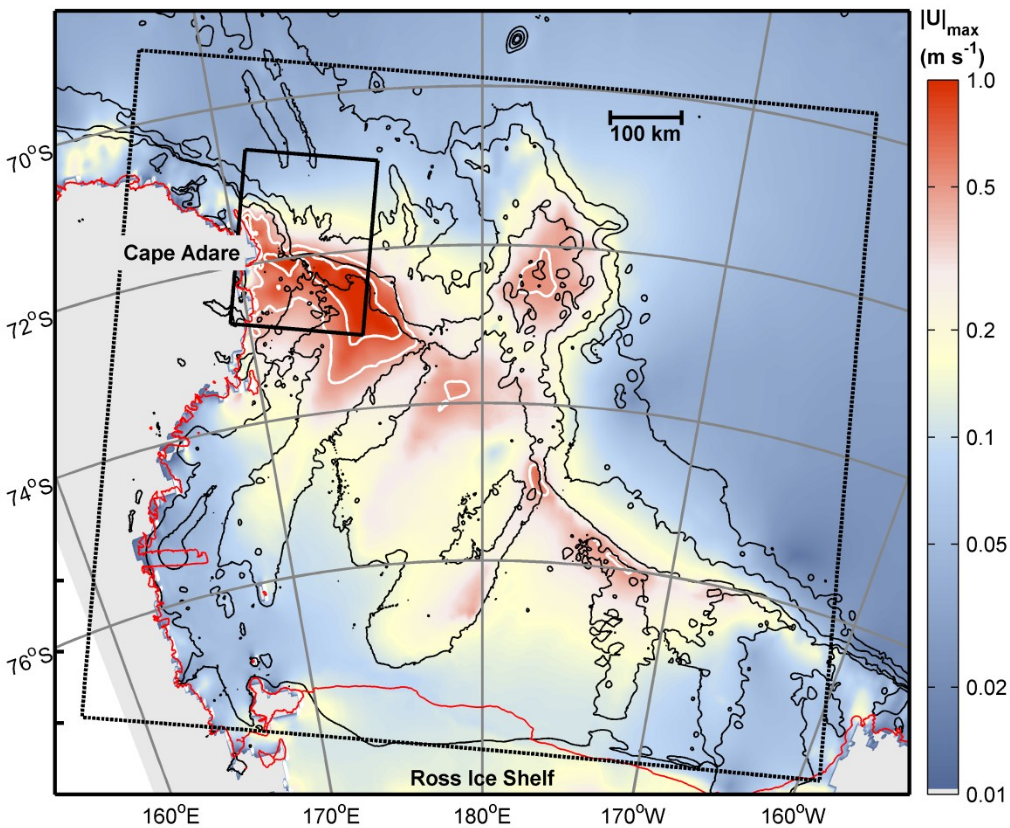

Figure 2: *Maximum tidal current speed* $|u|_{max}$ *(m* s^{-1}*) from a ten-constituent Ross Sea barotropic tide inverse model [Erofeeva et al., 2005]. Color scale is on right. The white contours along the shelf break show* $|u|_{max}$ *= 0.5 and 0.8m* s^{-1}*. Black contours show 500, 1000, 2000 and 3000-m isobaths. Red contour shows coastline and ice front from MODIS Mosaic of Antarctica. [Figure from Padman et al., 2009].*

The most relevant study to the present work is by *Erofeeva, Padman and Egbert* [2005], who assimilated current meter records and ADCP data from three cruises (between 1997 and 2003) in the Ross Sea. The primary region of the Ross Sea in which VM-ADCP assimilation has a significant impact is along the shelf break where tidal currents are large [*Whitworth and Orsi*, 2006; *Budillon et al.*, 2011]. While this is a small fraction of total Ross Sea area, it is where dense shelf water flows and mixes downslope to form Antarctic Bottom Water (AABW); based on 3-D numerical modeling, tides have a significant impact on formation rates [*Padman et al.*, 2009] there, motivating improvements in tide models. *Erofeeva et al*. [2005] showed that the fit between measured currents near the shelf break and models improved significantly when VM-ADCP data were assimilated.

The new VM-ADCP dataset is an order of magnitude larger, and much more spatially extensive, than that used by *Erofeeva et al*. [2005], prompting a re-evaluation of their use in inverse tide modeling. For this study we largely followed *Erofeeva et al.* [2005], except that we took advantage of new developments in treating the entanglement of the two closely-spaced (in frequency) diurnal constituents K_1 and P_1. Comparisons between maps of the major axis (U_{maj}) for the most energetic tidal harmonic O_1 (**Figure 3**) show the following:

- The expanded database allows resolution of much smaller-scale tidal variability than in the old VM-ADCP assimilation model, especially "hot-spots" of tidal energy along Antarctic Bottom Water (AABW) outflows along the western Ross Sea shelf break; and
- Change in predicted magnitude of tidal currents over troughs and banks running across the Ross Sea continental shelf.

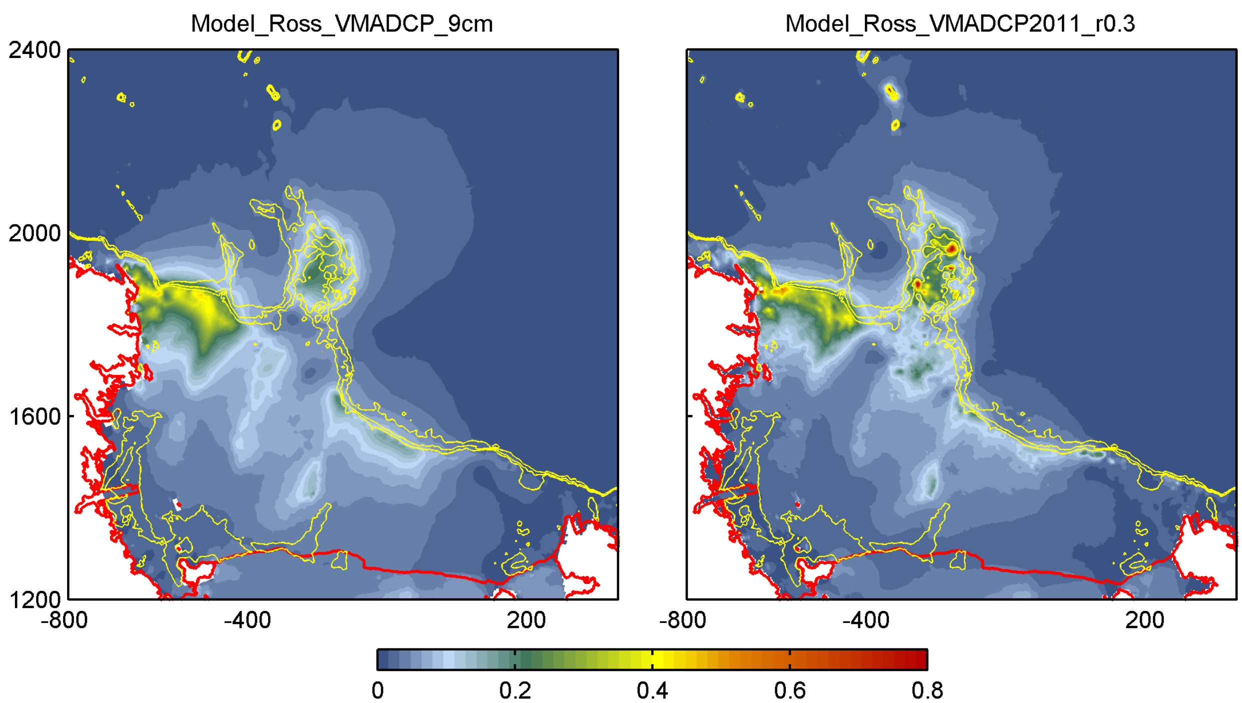

Figure 3: *Major axis U_{maj} (m s^{-1}) of O_1 diurnal tidal constituent from (left) original VMADCP assimilation model [Erofeeva et al., 2005] and new assimilation model using larger VM-ADCP database. Yellow contours show 700, 1000, and 1500 m isobaths. Red contour shows coastline and ice front from MODIS Mosaic of Antarctica.*

Comparison of the time-averaged tidal velocity maps, without and with tide corrections (**Figure 4**) reveals the importance of this correction. Most regions of apparently strong mean currents disappear, with the true residual circulation being <0.15 m s^{-1}. The sole exception is along the shelf break in the NW Ross Sea at the mouth of Drygalski Trough. A zoom of this region (**Figure 5, upper left**) shows a circulation that is generally consistent with expectations from moorings deployed during the AnSlope program [*Whitworth and Orsi*, 2006; *Gordon et al*., 2009]. However, the VMADCP provides broader spatial information, including an almost complete coverage of the Antarctic Slope Front (ASF) from east of Glomar Challenger Trough to Cape Adare, with typical speeds of 0.1-0.2 m s^{-1} (directed westward) with a width of ~10-20 km.

ESR has run several models of Ross Sea circulation using different combinations of forcing. Wind stress is derived from either the global, coarse-grid reanalysis product ERA-Interim or the medium-resolution Antarctic Mesoscale Prediction System (AMPS). Runs are also performed with and without tides. **Figure 5** compares time-averaged summer model fields with the VM-ADCP grid.
All models qualitatively capture the structure of the ASF, with strongest flows of ~0.3 m s^{-1} westward along the upper slope. The VM-ADCP record hints at a secondary circulation branch over the outer continental shelf about 50 km south of the shelf break; however, this is poorly resolved. A secondary branch is also seen in the AMPS runs (with and without tides); however, the direction of flow is reversed. The ERA-forced model without tides does not show this branch, generates too broad an ASF, and fails to capture the alongslope variations in ASF speeds seen in the VM-ADCP analysis and the AMPS-forced models. We are running alternative forcing products to see whether we can improve the match with VM-ADCP data.
Similar comparisons between VM-ADCP-derived mean fields and modeled summer fields for the McMurdo Sound region around Ross Island in the SW Ross Sea (**Figure 6**) again suggest that AMPS forcing (with or without tides) provides a better representation of upper-ocean currents than we get from the coarse-grid ERA_Interim product. The modeled current fields (with AMPS) are qualitatively similar to VM-ADCP; however, modeled currents are too weak. Observed southwestward flow around the NW tip of Ross Island is captured, as is the northward flow away from the ice-shelf front to the east of Ross Island. However, the strong northward flow measured along the Victoria Land coast west of Ross Island appears as a coastal-trapped current in the models, not extending as far east as the measured flow. This observation hints at more efficient outflow of near-surface waters from under the ice shelf, with consequences for sea-ice growth in the western Ross Sea.

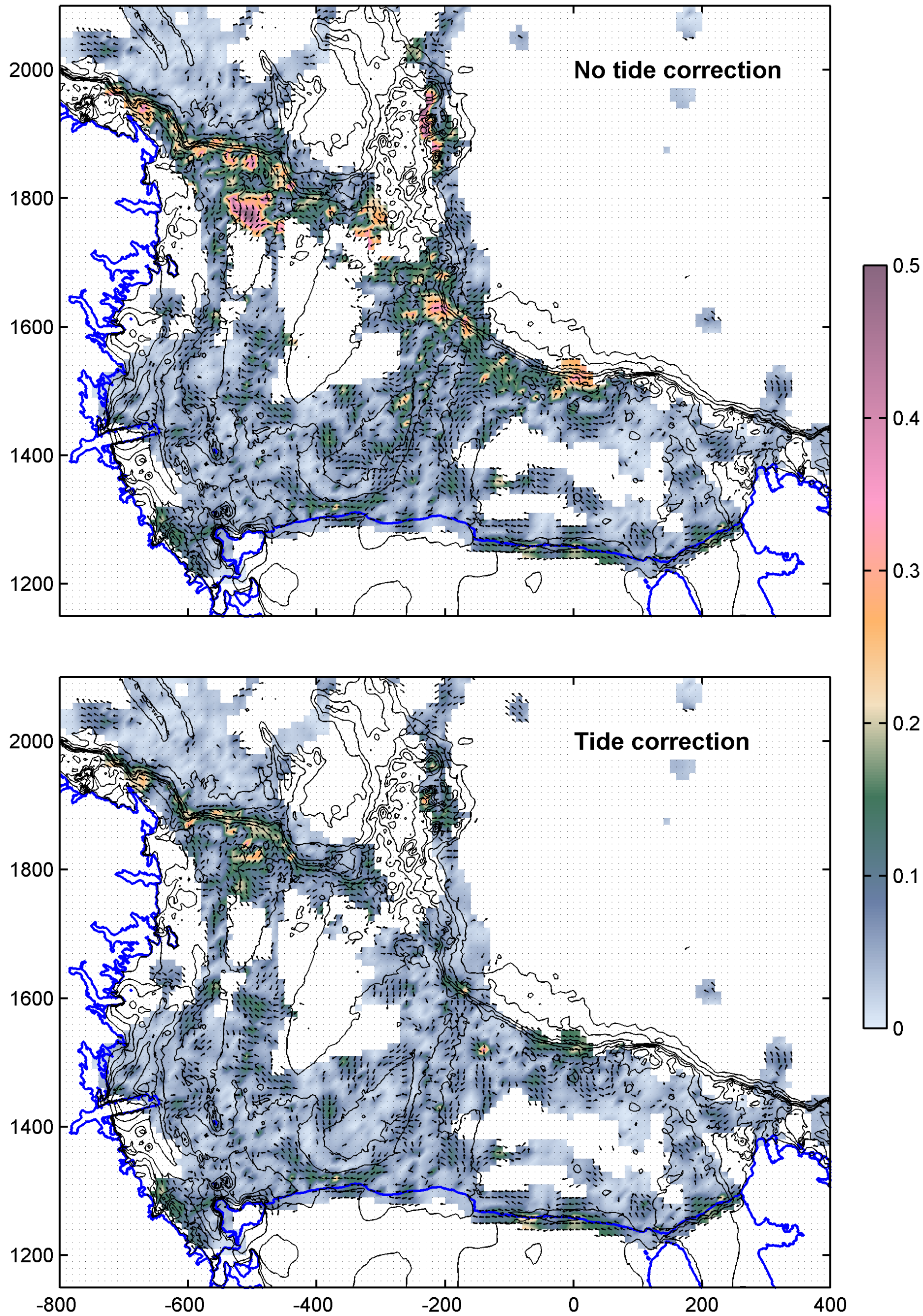

Figure 4: *Mean velocity (m s^-1^) in 10x10 km grid cells for NBP VM-ADCP currents averaged over 50-300 m depth. (top) no tide correction; (bottom) detided with most recent assimilation tide model. Colors show mean speed; unit vectors show direction for speeds >0.04 m s^-1^. Note significant reduction in velocity hot-spots along shelf break.*

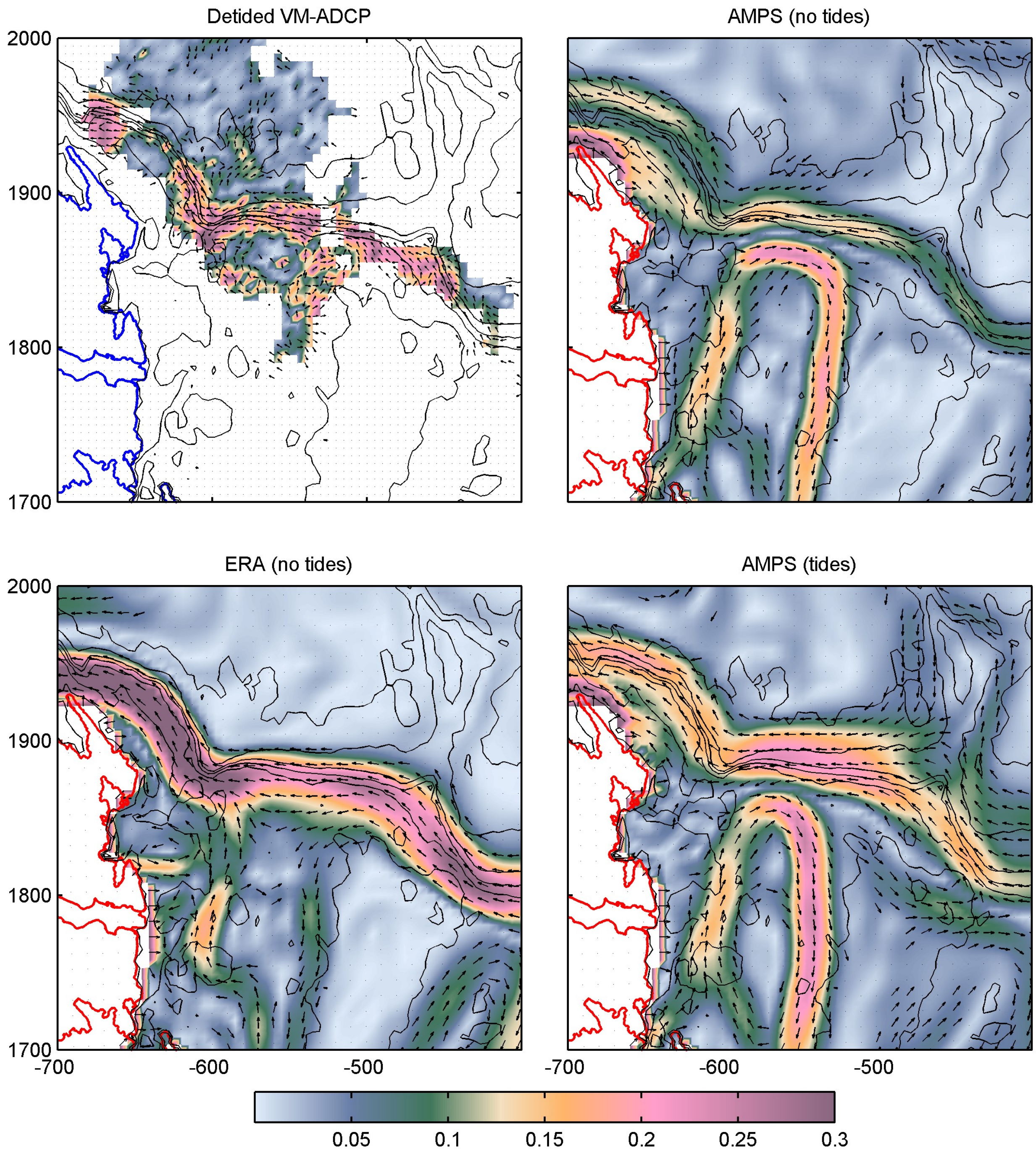

Figure 5: *Comparison of VM-ADCP averaged upper ocean (50-300 m) detided currents in the NW Ross Sea with summer 2005 fields from three models: AMPS-notides (upper right), AMPS-tides (lower right) and ERA-Interim-notides (lower left). Color shows speed; black unit vectors show direction. Comparison is with summer model fields since most VM-ADCP data were collected in summer. VM-ADCP averages are on a 5x5 km grid.*

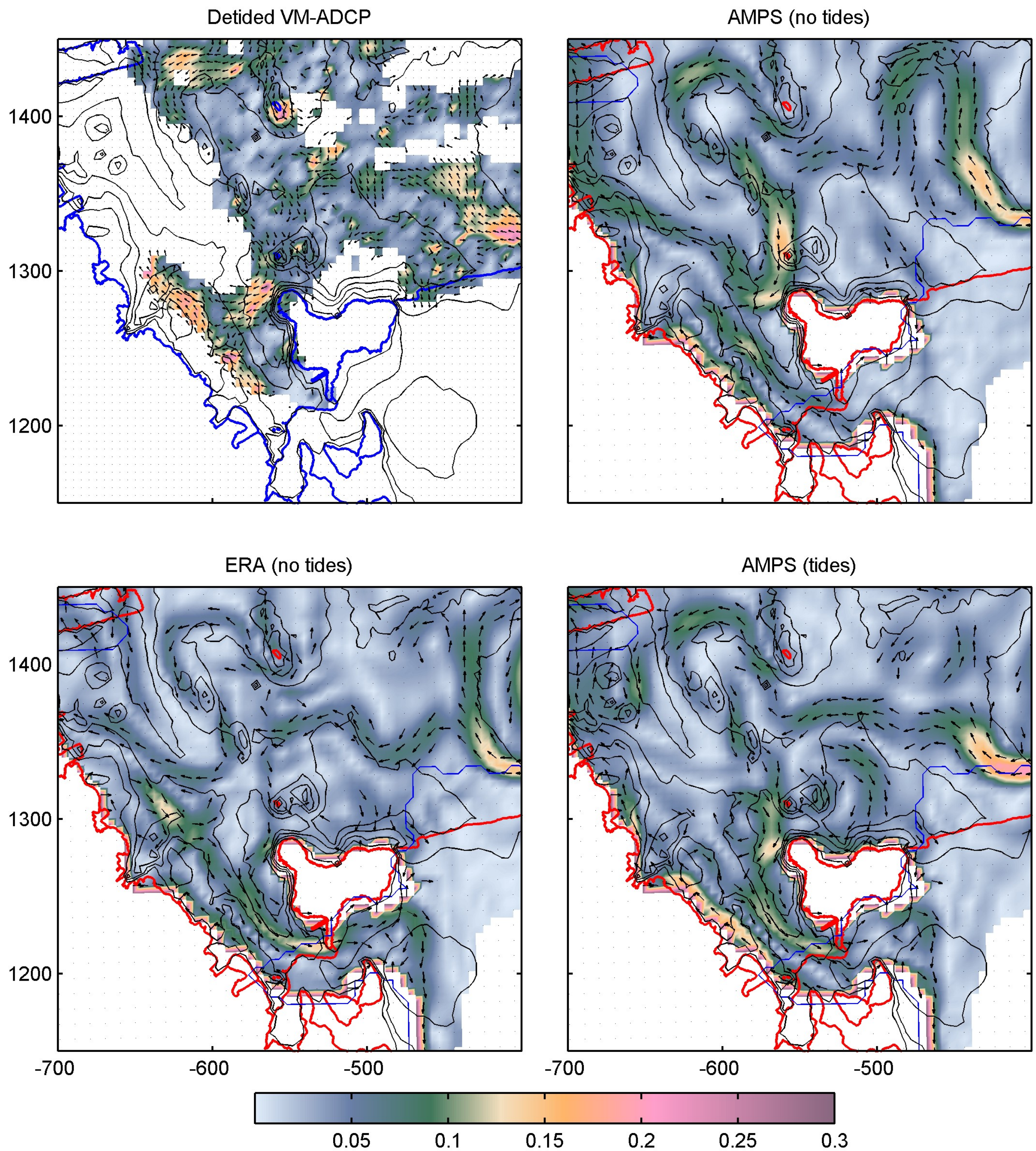

Figure 6: *Comparison of VM-ADCP averaged upper ocean (50-300 m) detided currents in and near McMurdo Sound with summer 2005 fields from three models: AMPS-notides (upper right), AMPS-tides (lower right) and ERA-Interim-notides (lower left). Color shows speed; black unit vectors show direction. Comparison is with summer model fields since most VM-ADCP data were collected in summer. VM-ADCP averages are on a 5x5 km grid.*

Towards a model for real-time detiding of VM-ADCP-derived currents

L. Padman's primary interest in tides is how they impact longer time-scale processes including AABW formation, sea-ice variability and ice-shelf basal melt rates, where tidal currents are critical components. However, most users of ESR's tide models merely want to detide signals. Over most of the last decade, the vast majority of users were only interested in heights, primarily for detiding altimetry over floating ice shelves. However, with lowered ADCP (LACDP) installations becoming more common on CTDs, and more reliable real-time currents available from VM-ADCPs, more users now require tidal current predictions. For this use, our prior approach of assimilating mostly height data is inadequate; it is possible to have a good inverse model for heights by assimilating heights, but the associated current field can be poor.

As an example, hot off the press, of real-time use of tide models, the recent (January 2012) NBP cruise in the Ross Sea has been using our older VM-ADCP assimilation tide model; see example provided by Dennis McGillicuddy in **Fig. 7**. Tides explain most of the upper-ocean currents measured by the VMADCP; real-time removal allows better identification of currents associated with other processes. In this case, the opposed flows either side of the 'X' in the tracklines represent southward and northward flows either side of the ridge of Ross Bank. Ridges across the Ross Sea play a profound role in delivering warm water to the Ross Ice Shelf front, and transporting dense shelf water formed in the western Ross Sea back to the shelf break [*Budillon et al.*, 2011 (incl. Padman), 2011].

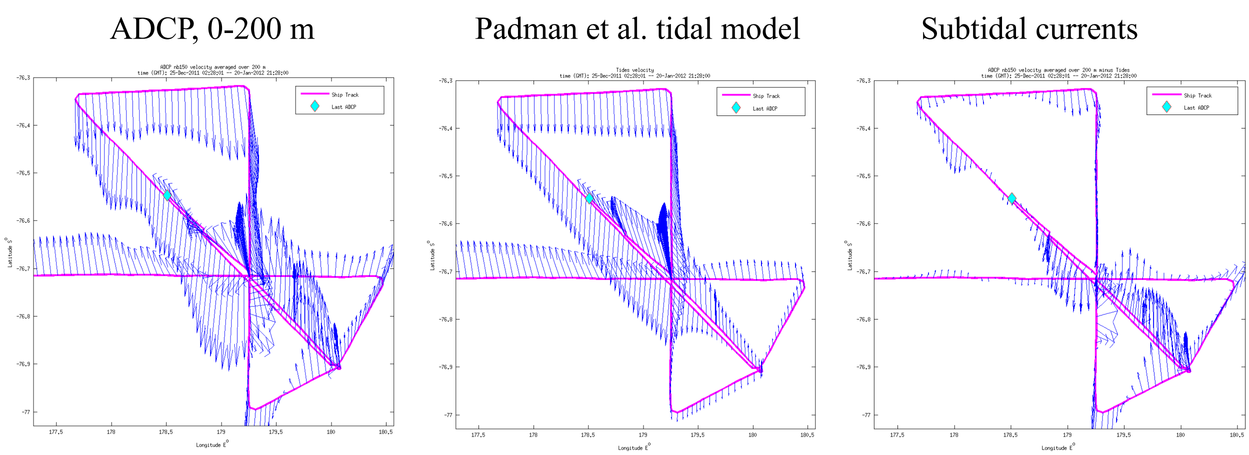

Figure 7: *NBP VM-ADCP, averaged over 0-200 m depth, for a survey over Ross Bank in the Ross Sea in January 2012 (courtesy D. McGillicuddy, 2012). Near real-time removal of tidal currents allows at-sea researchers to identify lower frequency features of ocean circulation for further study.*

A rigorous test of whether we are approaching a dynamically consistent tide model (heights and currents consistent with physics and geometry) is provided by validating the height-assimilation model with current data, or vice versa. In the NW Ross Sea where currents are large, we have only one tide gauge, a bottom pressure recorder from 2003/04 (AnSlope) [*Padman et al.*, 2009]. **Table 1** compares the O_1 amplitudes and phases for various tide models described above.

Table 1: *Comparison of tidal coefficients for O_1 for the AnSlope bottom pressure recorder mooring site [Padman et al., 2009], for four ESR barotropic tide models.*

O_1	Mooring analysis	CATS2008b*	VMADCP Prior (2011)	VMADCP Inverse (2011)	VMADCP Inverse (2005)
Amp (cm)	39.5	38.2	38.1	36.1	43.3
error	-	1.3	1.4	3.4	3.8
Phase	184.5	184.3	184.8	184.4	180.5
error	-	0.2	0.5	0.1	4.0

* CATS2008b assimilates this mooring data and so is not independent.

This comparison shows that VM-ADCP assimilation degrades the sea surface height amplitude fit for both the 2005 [*Erofeeva et al*., 2005] and updated models; however, tidal height phase is now very accurate. This is a typical result. We are using this information to develop methods to assimilate both height and current (VM-ADCP) data simultaneously.

Ross Ice Shelf ice front currents

Numerous cruises have collected VMADCP data from along the Ross Ice Shelf (RIS) ice front; green dots in **Figure 8** show locations of hourly averaged, detided 50-300 m averaged currents from all these cruises within 15 km of the ice front. By averaging these measurements in space (10x10 km gridding used here), we build up a map of mean ice front currents (**Figure 8a,c**). Speeds are up to 0.3 m s^{-1}. Currents are generally roughly parallel to the local ice front (towards the west), but there are some large cross-front components in a few locations (see near x=-100 and +200 km).

These cross-front current components identify areas of ventilation of the cavity under the RIS. Our models show some of this, with warmer water at specific locations; however, our models do not get the pronounced along-front components representing a general drift of ice-front water masses (including outflowing Ice Shelf Water) towards the west. All of our models fail to represent the persistent westward flow along the front of the RIS in the eastern Ross Sea. We tentatively conclude that the model numerical requirement for a sloping ice shelf front, rather than the more realistic "wall", interferes with the models' representation of currents above the depth of the real ice-shelf draft. We will be investigating this in new model runs at higher resolution that permit steeper modeled ice fronts.

Southern Ocean velocity structure

Several cruises crossed the Southern Ocean between Lyttelton NZ and the western Ross Sea (crossing the shelf break west of the dateline (180ºE/W). **Figure 9** shows a meridional transect occupied during the NBP0408 cruise returning to Lyttelton from AnSlope-3. For this entire transect, sea state was calm, and the OS38-NB acquired good data to >1000 m (and up to 1400 m). The high quality and rapid sampling by VM-ADCP (~1 nm spacing at 12 knots) provides detailed information on the spatial scale of fronts.

We have not pursued this study at this time, since the region is north of our model boundaries that target continental shelf processes.

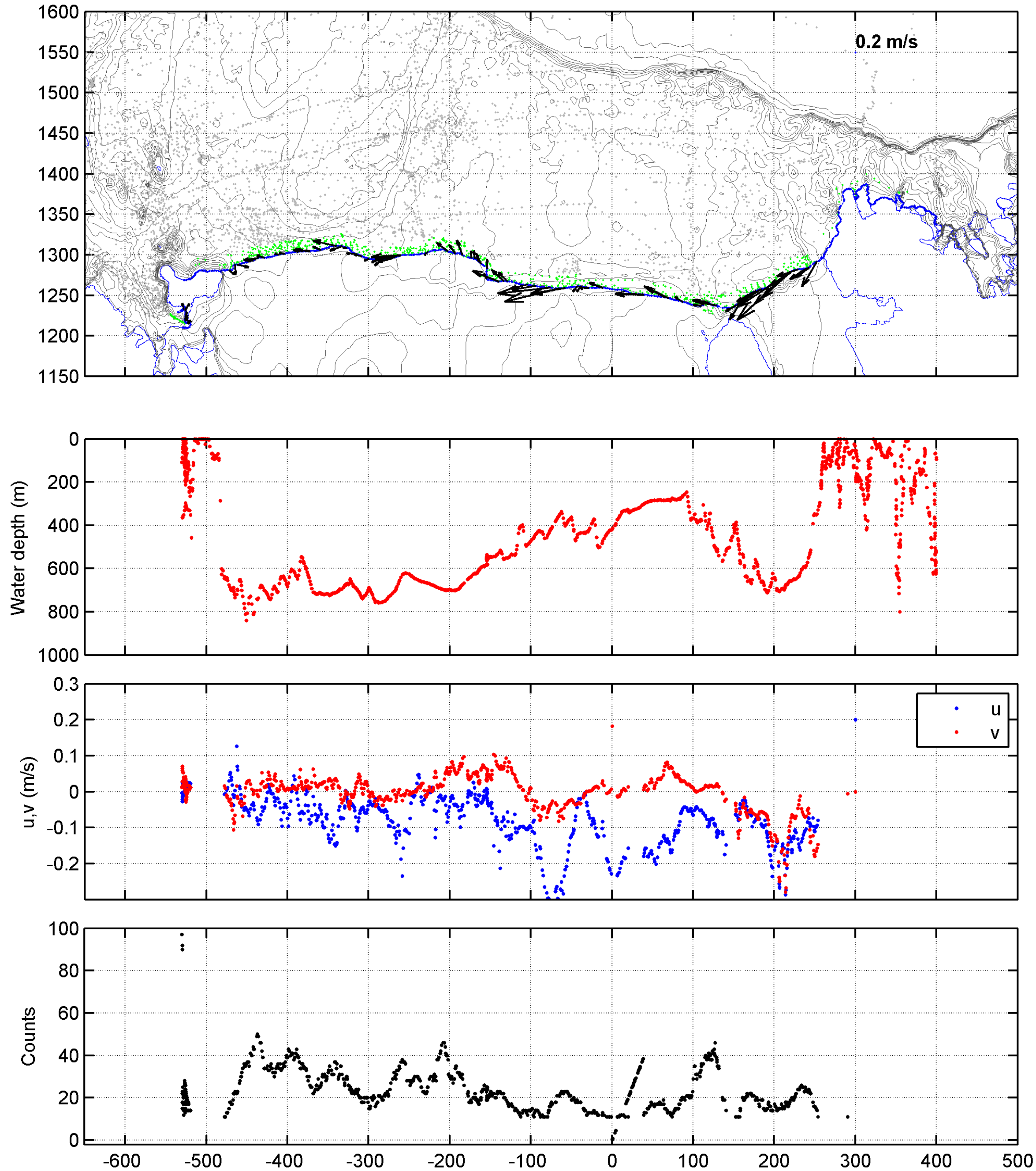

Figure 8: (a) Time-*averaged, detided velocity vectors from NBP VM-ADCP, averaged over 50-300 m depth, for all cruises along the ice front of the Ross Ice Shelf (RIS). Green dots show actual locations of measurements used to create this ice-front transect; gray dots show distribution of the full VM-ADCP database. (b) Water depth along the same transect. (c) u (E/W) and v (N/S) velocity components. (d) Counts (numbers of hourly VM-ACDP measurements) going into each average (quality control check).*

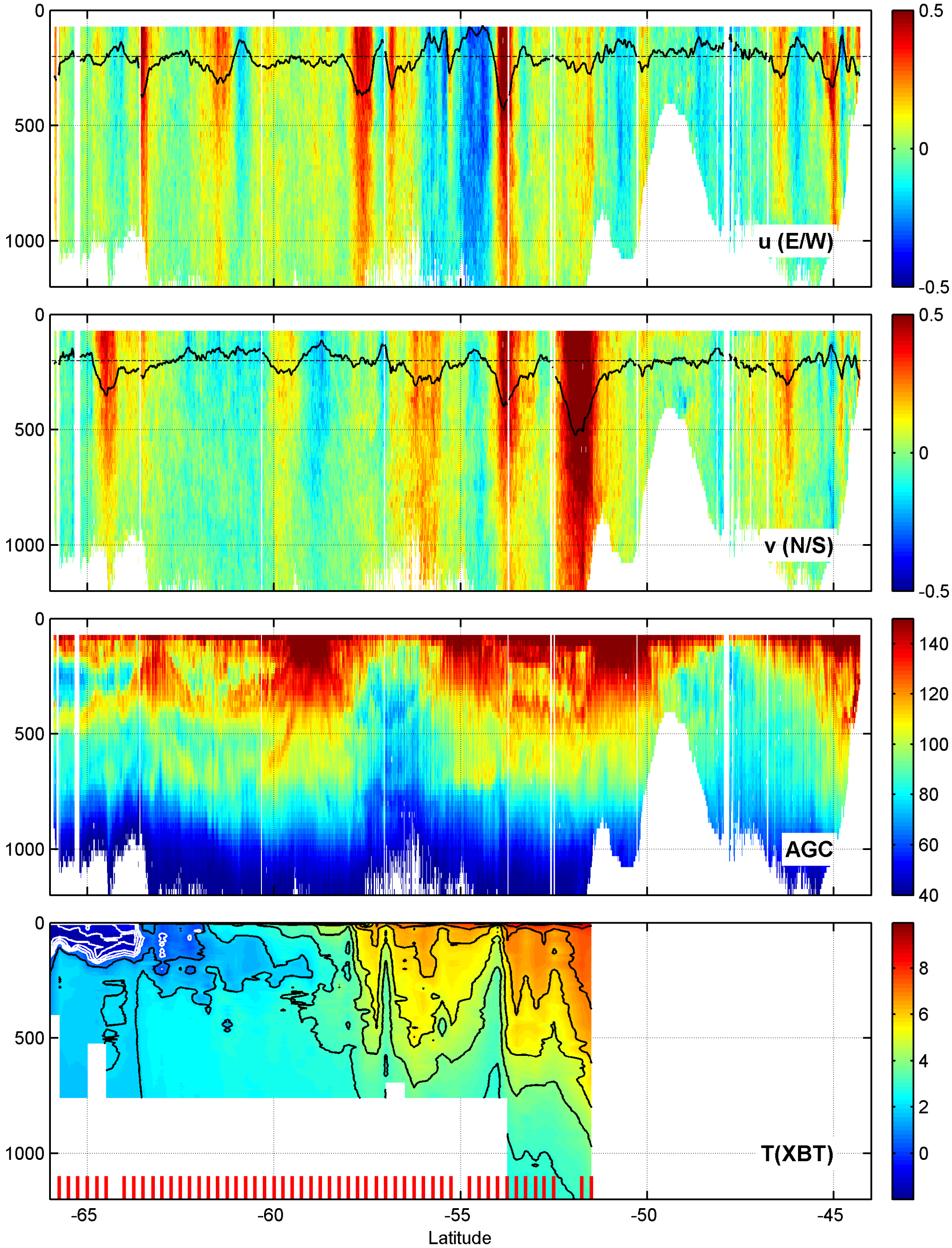

Figure 9: *Transects, as functions of latitude φ, for narrow-band OS38 products u(φ,z), v(φ,z) and backscatter amplitude (all sampled at 5 minutes), and temperature (from XBTs) on northbound leg of AnSlope 3 cruise NBP0408. Black lines on top two panels and offset and scaled mean velocity for 50400 m depth. Red ticks on bottom axis of bottom panel are locations of XBTs.*

Antarctic Slope Front (ASF)

The ASF is the dynamic boundary between the cold, dense shelf water masses and the warmer "offshore" water masses including Circumpolar Deep Water (CDW), the source of most ocean heat flowing onto the Ross Sea continental shelf. The ASF is routinely seen in hydrographic transects across the continental slope. However, it's location can vary from mid-slope to slightly inshore of the shelf break [*Budillon et al*., 2011], affected by wind stress and tides. The ASF appears to operate as a "flapper valve", allowing intermittent spillage of dense water offshore to contribute to AABW, and pulses of CDW and Modified CDW (MCDW) onshore.

Rapid variability of ASF position, combined with the time it takes to do CTD profiles, leads to aliasing of the ASF in transects. As a consequence, we don't have a good sense of how wide the Ross Sea ASF really is. However, the dynamic stability of a front depends, in part, on the magnitude of spatial gradients. **Figure 5** shows the time-averaged Antarctic Slope Current (the velocity expression of the ASF) in the NW Ross Sea based on the VM-ADCP database and three of ESR's Ross Sea models. However, as *Budillon et al.* [2011] pointed out, time averaging smears out the ASF (and the ASC).

The rapid sampling rate of the VM-ADCP (5 minutes) implies the ability to resolve the ASC to ~1 km assuming 12 knots ship speed (no ice). The entire ASC is ~20 km wide (Figure 5), so that it can be sampled in ~1 h under ice-free conditions. (Detailed transects in AnSlope were hampered by thick ice, so that VM-ADCP were only acquired at CTD stations.)

A total of 17 cruises in the VM-ADCP database contained transects crossing the Ross Sea shelf break. Most of these were along the western sector between Cape Adare and Glomar Challenger Trough: however, two cruises (NBP9901 and NBP9909) crossed the eastern continental slope in 1999. Only a few of these were in ice-free conditions without stopping for sampling activities. Nevertheless, they provide valuable information about the ASC position and intensity. We describe two examples here.

NBP0305A crossed the slope at the Drygalski Trough sill in late December 2003 (**Figure 11**). A strong, narrow westward jet >0.5 m s^{-1} is centered over the shelf break (t=359.6 in the figure). However, the velocity field is complex: even after detiding, large eastward velocities are found south of the shelf break. These lend support to the modeled circulation (**Figure 5**), especially runs forced with AMPS winds and with tides. This transect is unusually baroclinic, which we attribute to the large tides (>0.5 m s^{-1}) predicted at the time of crossing the continental slope; cf. *Padman et al.* [2009], their Figure 11.

NBP0602 crossed the slope on the eastern side of Iselin Bank sill three times in early February 2006 (**Figure 12**). In this case the "Ocean Surveyor" long-range VM-ADCP was operational and measured currents up to 1200 m depth. The first transect (t=33.8-34 in Figure 12) crosses where the dense outflow from the Glomar Challenger Trough is flowing along the continental slope [*Budillon et al*., 2011]). There is a narrow, strong current at the top of the slope (t=33.8) directed southeast, opposite the expected direction of the ASC. In our models, only AMPS+tides shows any hint of this counter-current in this region. However, bathymetry data are relatively sparse here, and flows are strongly influenced by even quite subtle changes in bathymetry. Unfortunately, the acoustic dead-zone within ~100 m of the seabed prevents us from seeing the dense outflow from Glomar Challenger Trough, even if it is within the sampled region (water depths less than ~1000 m).

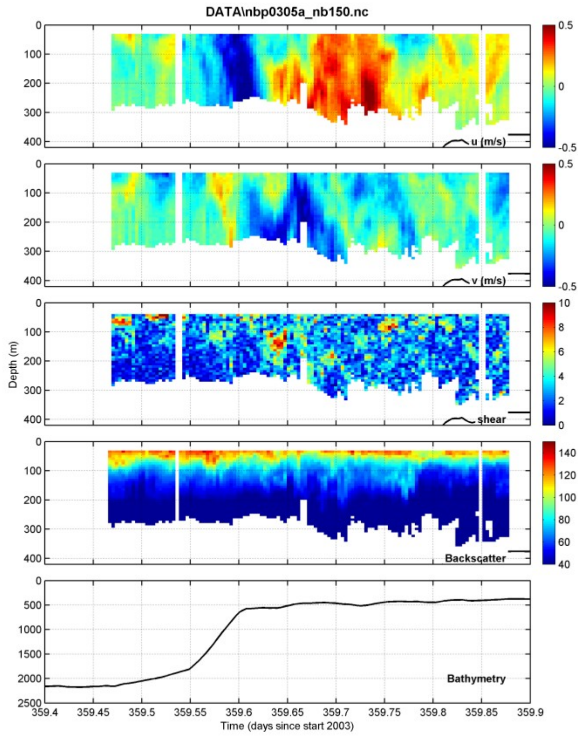

Figure 10: *Transects across slope north of Drygalski Trough, as functions of time, for NB150 products u(t,z), v(t,z), scaled shear, and backscatter amplitude (all sampled at 5 minutes), from NBP0305a.*

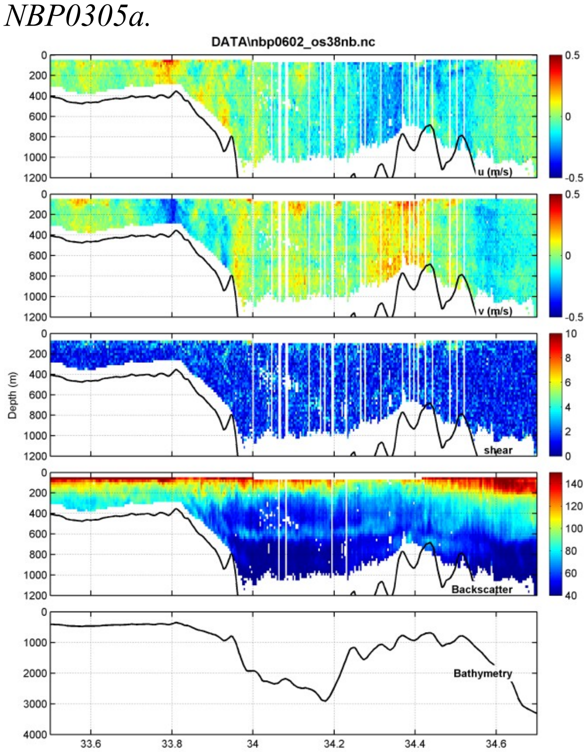

Figure 11: *Transects across slope of Iselin Bank north of Glomar Challenger Trough, as functions of time, for NB 38 kHz products u(t,z), v(t,z), scaled shear, and backscatter amplitude (all sampled at 5 minutes), from NBP0602.*

Cited References

Budillon, G., P. Castagno, S. Aliani, G. Spezie, and L. Padman (2011), Thermohaline variability and Antarctic Bottom Water Formation at the Ross Sea shelf break, *Deep-Sea Res. I* , *58*, 1002-1018.

Erofeeva, S. Y., G. D. Egbert, and L. Padman (2005), Assimilation of ship-mounted ADCP data for barotropic tides: Application to the Ross Sea, *J. Atmos. Oceanic Technol.*, *22*(6), 721-734.

Padman, L., L. Erofeeva, and H. A. Fricker (2008), Improving Antarctic tide models by assimilation of ICESat laser altimetry over ice shelves, *Geophys. Res. Lett.*, *35*, L22504, doi:10.1029/2008GL035592.

Padman, L., S. Erofeeva, and I. Joughin (2003), Tides of the Ross Sea and Ross Ice Shelf cavity, *Antarct. Sci.*, *15*(01), 31-40.

Padman, L., and H. A. Fricker (2005), Tides on the Ross Ice Shelf observed with ICESat, *Geophys. Res. Lett.*, *32*, L14503, doi:10.1029/2005GL023214.

Padman, L., H. A. Fricker, R. Coleman, S. Howard, and S. Erofeeva (2002), A new tidal model for the Antarctic ice shelves and seas, *Ann. Glaciol.*, *34*, 247-254.

Padman, L., S. L. Howard, A. Orsi, and R. Muench (2009), Tides of the northwestern Ross Sea and their impact on dense outflows of Antarctic Bottom Water, *Deep-Sea Res. II*, *56*, 818-834, doi: 10.1016/j.dsr2.2008.10.026.